Vol. 90 (1996) *ACTA PHYSICA POLONICA A* No. 4

Proceedings of the XXV International School of Semiconducting Compounds, Jaszowiec 1996

SHALLOW DONORS AND ACCEPTORS IN GaN; BOUND EXCITONS AND PAIR SPECTRA

R. STĘPNIEWSKI AND A. WYSMOLEK

Institute of Experimental Physics, University of Warsaw
Hoża 69, 00-681 Warsaw, Poland

Recent photoluminescence results obtained for homoepitaxial GaN layers are presented. Dominant photoluminescence structures observed for these layers can be assigned to excitons bound to neutral impurities. Different methods such as temperature dependent evolution, high magnetic field and time resolved spectroscopy have been used to study the exciton line properties. For the p-type samples sharp lines are observed, assigned to the donor–acceptor recombination for differently distant pairs. The analysis of the optical transitions related to donors and acceptors is in reasonable agreement with the effective mass approximation. Electron phonon interaction was found to strongly affect the optical properties of GaN. The dominant intrinsic defect has been identified as a donor located at a nitrogen site.

PACS numbers: 71.35.–y, 71.55.Eq, 71.38.+i

1. Introduction

Gallium nitride is one of the most promising materials for potential applications in short wavelength optoelectronics and high temperature devices. The basic physical knowledge about this material is still not satisfactory. Fundamental studies are limited by the unsatisfactory quality of the samples. The major problem that has slowed down the development of technology was the lack of good quality, lattice matched substrates for MOCVD epitaxy.

Homoepitaxial GaN MOCVD layers have been grown only recently [1,2]. GaN monocrystal plates, which were used as substrates, were grown from a dilute solution of atomic nitrogen in liquid gallium at a temperature of 1600°C and a nitrogen pressure of about 15–20 kbar [3]. Crystals grown by this method are in the form of platelets with the hexagonal c [0001] axis perpendicular to the surface. The growth of GaN single crystals and the properties of homoepitaxial layers were reported in Refs. [4] and [5]. The stress in such MOCVD layers is small ($\Delta c/c < 2 \times 10^{-4}$), as verified by X-ray measurements [6]. Luminescence and reflectivity results [7] reveal their good optical properties. Optical studies of such samples give new insight into the band energy structure and the nature of the impurities which dominate the optical properties of this material.

1.1. Basic properties of GaN

Gallium nitride is a III–V compound that crystallises in the wurtzite structure with the lattice parameters (relaxed homoepitaxial layer at 300 K): $a = 3.1878(3)$ Å and $c = 5.1850(2)$ Å [6]. The ratio $c/a = 1.6265$ is very close to the value of an ideal wurtzite structure $(c/a)^{\mathrm{id}} = \sqrt{8/3} \approx 1.6330$. The Ga–N distances are of equal length and only the bond angles deviate from the values for a regular tetrahedron [8]. It has been demonstrated [9] that an epitaxial metastable zinc-blende structure β-GaN, with a lattice constant of $a_0 = 4.511$ Å [6], can also be grown. One can notice the same interatomic distances found for both phases (within experimental error $a\sqrt{2}/a_0 = 1$). The generally accepted band structure of cubic [10] and hexagonal [11] GaN has been confirmed by spectroscopic elipsometry studies at photon energies up to 25 eV [12].

1.2. Free exciton structure

Both in the zinc-blende and the wurtzite structure, GaN is a direct band gap semiconductor. The optical energy gap E_0 for the cubic phase is determined by the free exciton built from a free electron from the Γ_6 conduction band and a free hole from the Γ_8 valence band. E_0 was found to vary from $E_{g0}^{c} = 3.302(4)$ eV at 10 K to 3.231(8) eV at 300 K, and the spin–orbit splitting between the Γ_8 and Γ_7 valence bands was determined to be $\Delta_0 = 17(1)$ meV [13].

For GaN in the wurtzite structure, the crystal field splitting removes the heavy-light hole degeneracy of the Γ_8 band. It is generally accepted that the Γ_9 valence band is located on top, as in CdS [14]. Three excitons A, B and C (Fig. 1), which correspond to the split valence bands of Γ_9, Γ_7 and Γ_7 symmetries, can be observed in reflectivity, and can give rise to photoluminescence*.

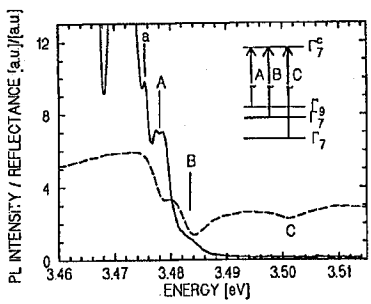

Fig. 1. The free exciton transitions observed in the luminescence (solid line) and reflectance (dashed line), as measured at temperature 4.2 K for the same sample.

For GaN homoepitaxial layers it was found that E_A varies from 3.4776(3) eV at 4.2 K to 3.412(1) eV at 300 K [15]. At low temperature B and C exciton lines were found at energies $E_B = 3.4827(3)$ eV and $E_C = 3.5015(20)$ eV. The relation

*The observation of the exciton C in photoluminecence was reported in Ref. [18].

between the valence band energies for the wurtzite structure is described by the following equation [16]:

$$E_1 - E_{2,3} = \frac{1}{2}\left[(\Delta_1 + 3\Delta_2) \mp \sqrt{(\Delta_1 - \Delta_2)^2 + 8\Delta_3^2}\right], \tag{1}$$

where Δ_1 — crystal field, Δ_2 and Δ_3 — parallel and transverse spin–orbit splitting parameters, and E_1, E_2, E_3 correspond to the Γ_9, Γ_7 and Γ_7 bands, respectively.

It is impossible to estimate Δ_1, Δ_2 and Δ_3 only on the basis of the observed splittings. As it was mentioned above, GaN has an almost ideal wurtzite structure, and therefore the quasi-cubic model [16] can be used to approximate the valence band structure. Within this approximation

$$\Delta_1 = \Delta_{cr}, \qquad \Delta_2 = \Delta_3 = \Delta_{so}/3 \quad \text{and}$$

$$E_1 - E_{2,3} = \frac{1}{2}\left[(\Delta_{cr} + \Delta_{so}) \mp \sqrt{(\Delta_{cr} + \Delta_{so})^2 - \frac{8}{3}\Delta_{cr}\Delta_{so}}\right], \tag{2}$$

where Δ_{cr} — crystal field and Δ_{so} — spin–orbit splitting.

Neglecting the possible differences in the A, B, C exciton binding energies, one can obtain the following values for stress free, homoepitaxial GaN: $\Delta_{cr} = 9.3(3)$ meV and $\Delta_{so} = 19.7(1.5)$ meV [15].

Most of the published data has been obtained using good quality GaN epitaxial layers grown on sapphire or SiC substrates using MOCVD, HVPE or MBE technologies. Due to the large lattice mismatch between the substrate and GaN layer, the optical properties are affected by the strain present in such samples [17, 18].

The binding energy of exciton A in GaN has been experimentally estimated to be $E_X = 26.7$ meV [18], which (surprisingly in Ref. [19] the electron effective mass (polaron mass) $m^* = 0.19$ was used) is in good agreement with theoretical predictions of (27.7 meV) [19]. Using this value, the low temperature energy gap of GaN $E_g = 3.504(1)$ eV can be derived.

1.3. Shallow impurities within the effective mass approximation

The conduction band electron effective mass (polaron mass) has been determined by cyclotron resonance experiments [20, 21]: $m_e^* = 0.22$. The binding energy of the shallow hydrogen-like donor can be predicted (in the weak electron–phonon interaction limit) to be $E_D^B = 31.8$ meV. However, taking into account the value of the electron–phonon coupling constant $\alpha_e = 0.44$ [22], which locates GaN close to the intermediate interaction range, the textbook formula [23] gives $E_D^B = 65$ meV. For the effective mass ratio $m_h^*/m_e^* = 3.4$ ($m_h^* = 0.75$ was taken after Ref. [18]) the binding energy of the exciton bound to the neutral donor complex can be estimated [24] to be $E_{XD}^B = 0.12E_D^B = 3.8$ meV or 7.8 meV, respectively.

In the case of acceptor-related complexes, one should take into account more accurately the complicated valence band structure, since $E_A^B \gg \Delta_{cr}, \Delta_{so}$. In the crude approximation for a free hole with a polaron mass value $m_h^* = 0.75$ one can estimate the electron phonon coupling constant to be equal to $\alpha_h = 0.77$. Since $\alpha_h > 0.5$, it is rather the intermediate range of electron–phonon interaction which should be applied, leading to the acceptor binding energy [23] $E_A^B \approx 210$ meV (the

weak coupling limit gives 110 meV). The binding energy of the exciton bound to the neutral acceptor can be obtained [24] as $E^{B}_{XA} = 0.06E^{B}_{A} = 12.6$ meV. One can see that to describe the shallow impurities in GaN a proper treatment of the electron–phonon interaction is crucial. In the case of acceptors also the valence band structure has to be taken into account. To the best of our knowledge, such an analysis has not been yet performed.

2. Experimental results

2.1. Luminescence in the exciton region of homoepitaxial GaN

Luminescence and reflectivity in the exciton region of undoped homoepitaxial GaN layers (discussed in detail in Ref. [7]) is shown in Fig. 2. The low temperature spectrum is dominated by two strong and narrow lines: XD and XA at energies $E_{XD} = 3.4719$ eV and $E_{XA} = 3.4666$ eV. The FWHM of these lines are about 1.8 meV and 1.0 meV, respectively. The absolute values of the optical transition energies discussed in this paper are slightly sample dependent (within the range of 1 meV), however, the separation between the particular lines remains constant.

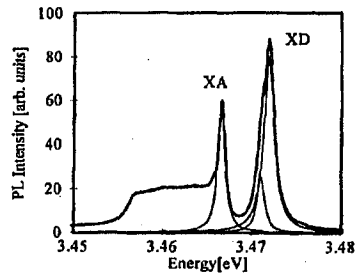

Fig. 2. The luminescence spectrum of homoepitaxial GaN in the exciton region, measured at 3 K.

The XA line is assigned to an exciton bound to a neutral acceptor (see below). The higher energy XD line for this sample shows a double peak structure which is well fitted with Lorentzian curves (Fig. 2), giving the following peak parameters: $E_1 = 3.4711$ eV, $E_2 = 3.4720$ eV, $\Gamma_1 = \Gamma_2 = 0.7$ meV. The relative intensities of these lines are different for different samples. We have assigned these lines to excitons bound to neutral donors. The XA line dominates the luminescence spectrum for p-type homoepitaxial layers doped with magnesium [25].

The binding energy of the acceptor bound exciton complex $E^{B}_{XA} = E_A - E_{XA} = 11.4(5)$ meV is in reasonable agreement with the theoretical estimation [24] (see Sec. 1.3). The value of the donor bound exciton localization energy $E^{B}_{XD} = E_A - E_{XD} = 6.0(5)$ meV is also located in the estimated range.

The origin of the weak line a (Fig. 1) is not clear. It can be associated with a donor bound exciton formed with the participation of a hole from the deeper Γ_7 valence band [7]. Due to the small splitting of the valence band, smaller than the optical phonon energy, the nonradiative relaxation from this state is strongly

suppressed. Two lines related to exciton B: free and bound to the neutral donor, can be observed in luminescence.

In Ref. [18] line *a* is ascribed to an exciton bound to another neutral donor. For such a donor one should have a positive, instead of a negative, central cell correction.

2.2. Luminescence in high magnetic fields

Magnetoluminescence has been measured at the High Magnetic Field Laboratory in Grenoble in a magnetic field up to 14 T in the helium temperature range [26]. In the Voight configuration, with a magnetic field perpendicular to the hexagonal axis ($\boldsymbol{B} \perp \boldsymbol{c}$), a splitting of the XA and XD lines occurs (Fig. 3). With increasing magnetic field strength the intensity of the high energy component of line XA decreases, whereas the components of the XD line remain almost unchanged. In a magnetic field perpendicular to the c axis, the initial state of the exciton bound to the neutral donor does not split [27]. The splitting observed in luminescence is caused by the splitting of the final state (neutral donor), and depends on the g value for the electron in the conduction band. In this case one cannot expect any differences in the intensities for two Zeeman split components. For the exciton bound to the neutral acceptor the opposite situation is true: the splitting occurs for the initial state involved in the luminescence and different occupations of the split components occur. Thus, a decrease in the intensity of the high energy component of the split line is observed. The dependences observed for lines XA and XD (Fig. 3) allow us to interpret them as the recombination of the exciton bound to a neutral acceptor and the exciton bound to a neutral donor, respectively.

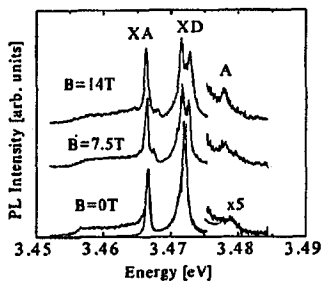

Fig. 3. The magnetic field evolution of the luminescence spectrum in the exciton region, measured at 3 K.

For the magnetic field $\boldsymbol{B} \perp \boldsymbol{c}$ the exciton line splitting should be related, in the first approximation, to the spin splitting of the conduction band [27]. The splitting of the observed lines is different for XA and XD (Fig. 4). The linear approximation of the observed splitting

$$\Delta E = g^* \mu_B B \tag{3}$$

allows us to evaluate the effective g^*-factors: $g^*_{XD} = 1.708 \pm 0.025$ and $g^*_{XA} = 2.040 \pm 0.015$, respectively, for the exciton bound to the neutral donor and acceptor.

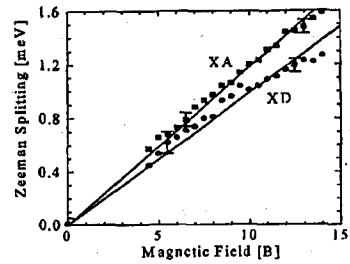

Fig. 4. The observed Zeeman splitting of the luminescence related to the exciton bound to the neutral donor (XD) and neutral acceptor (XA), as a function of the magnetic field. Solid lines — fitted according to Eq. (3).

At low magnetic fields, the g^*-factor in GaN was estimated from the ESR [28] and ODMR [29] experiments. Our high field estimation of $g^*_{XD} = 1.71$ is smaller than the value $g^*_e = 1.95$ obtained from the ESR and ODMR measurements. From the Zeeman effect on the exciton bound to neutral acceptor we obtain $g^*_{XA} = 2.04$. Increased values of the g^*-factor for deeply bound excitons were also reported in ODMR studies [29].

For the magnetic field parallel to the c-axis, the Zeeman splitting of bound excitons is too small to be detected. By analogy to the case of CdS [27], this can be understood as a result of the opposite Zeeman contribution in the conduction and the valence bands which almost exactly cancels the spin splitting of excitons.

2.3. Temperature dependence of the bound exciton luminescence

The temperature dependence of the luminescence spectrum in the exciton region is shown in Fig. 5. In spite of the fact that the XA line is at a larger distance from the free exciton than XD, this spectrum disappears first (above 40 K). The observed behaviour can be understood by taking exciton kinetic processes into account. Time-resolved photoluminescence experiments were performed on Mg doped GaN homoepitaxial layers [30]. It was found that the XD and XA lines show a decay time of about 90 ps and 700 ps, respectively. At higher temperature (35 K) the whole edge part of the photoluminescence has the same decay time

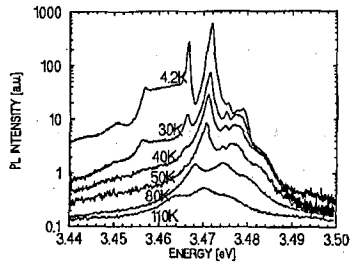

Fig. 5. The temperature evolution of the luminescence intensity in the exciton region.

as the free exciton emission. It has been postulated that temperature induced tunnelling from a neutral acceptor bound exciton to the donor bound one, as well as to a free exciton, takes place and allows a much faster exciton decay. As a consequence of this process, the DC photoluminescence intensity of the XA line rapidly decreases [31] with increasing temperature.

2.4. Donor acceptor pair recombination

For *p*-type homoepitaxial layers doped with magnesium, in addition to the strong excitonic structures XD and XA, there is also a group of lines close to 3.4 eV. This luminescence spectrum consists of more than 20 sharp lines of half width close to 1 meV (see Fig. 6). Discrete lines from the lower energy side are superimposed on the slope of the broad peak located at an energy of 3.266 eV. The middle part of the spectrum is affected by the LO phonon replica of exciton luminescence (see Fig. 6). By subtracting this additional structure it is possible to obtain a "pure" spectrum connected with donor–acceptor pair transitions [25,32].

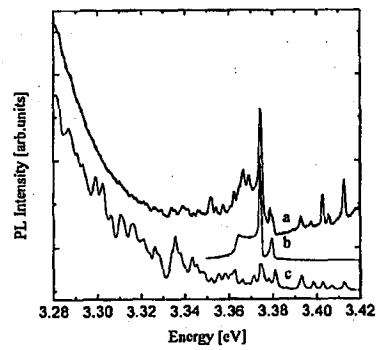

Fig. 6. (a) The fine structure of donor–acceptor emission measured at 4.2 K. (b) The bound exciton emission, shifted by the LO phonon energy in order to visualise its presence in the spectrum. (c) The calculated donor–acceptor spectrum.

The energy released as a photon when a hole on an acceptor recombines with an electron on a donor is approximately (neglecting the van der Waals interaction)

$$E_n = E_g - E_D - E_A + \frac{e^2}{\varepsilon_0 R_n}, \tag{4}$$

where E_g, E_D and E_A are the energy gap, the donor and the acceptor ionization energies, respectively, ε_0 is the static dielectric constant and R_n is the donor–acceptor separation. The attractive Coulomb interaction between the positively charged donor core and the negatively charged acceptor core, created after recombination, increases the energy of the transition by the last term of expression (4). The plot of the energy of the donor–acceptor transitions E_n versus $1/R_n$ should give a straight line with a slope determined by the static dielectric constant. Further information which may be obtained from this plot is the sum of the isolated donor and acceptor energies, which is determined by the limiting value of E_n for $R_n \to \infty$. By fitting a

straight line to the experimental data a value of the static dielectric constant equal to 9.6(1) and the limiting energy value of $E_n = 3.210(10)$ eV were obtained [25]. Assuming that the band gap energy $E_g = 3.504$ (Sec. 1.2), the sum of the isolated donor and acceptor binding energies of 294(10) meV can be obtained. The result of intensity calculations [25] is shown in Fig. 6. The line with the highest energy corresponds to a donor–acceptor separation equal to 7.13 Å. The best fit was obtained for the so-called type II spectra, when one impurity occupies a Ga site and the other an N site. Assuming that Mg occupies Ga lattice sites, donors involved in the pair spectra should be located on N sites. Such a result is in agreement with the assumption that a nitrogen vacancy is the main native shallow donor in GaN [33]. Temperature studies of the luminescence spectra reveal that in addition to donor–acceptor pair spectra it is possible to resolve the direct conduction band to acceptor emission. This observation allows us to estimate separately the ionization energy of the residual donor present in homoepitaxial layer at 55(15) meV and of the Mg acceptor at 235(15) meV [32].

3. Conclusions

Recent progress in homoepitaxial growth of GaN layers by MOCVD technology gives an access to high quality, almost stress free samples. Such samples have been used to study the basic optical properties of GaN. It has been found that luminescence spectra are dominated by bound exciton recombination. For magnesium doped homoepitaxial layers donor–acceptor pair spectra have been observed for the first time in GaN. The dominant intrinsic defect present in homoepitaxial layers has been identified as a donor located at the nitrogen site and can be related to the nitrogen vacancy. The donor and acceptor binding energy, as well as the binding energy of the excitons localised at these centres, are in reasonable agreement with the effective mass approximation, including the electron phonon interaction. A more accurate analysis, taking into account the complex valence band structure and electron–phonon interaction should be performed to make a detailed comparison between experimental results and theoretical predictions possible.

Acknowledgments

This work has been partially supported by the Committee for Scientific Research (Poland) grant 7 T08 A 06110 and the European Community grant CIPA-CT93-0161.

References

[1] K. Pakuła, J.M. Baranowski, R. Stępniewski, A. Wysmołek, I. Grzegory, J. Jun, M. Sawicki, S. Porowski, K. Starowieyski, *Acta Phys. Pol.* **88**, 861 (1995).

[2] K. Pakuła, J.M. Baranowski, R. Stępniewski, A. Wysmołek, I. Grzegory, M. Boćkowski, G. Nowak, M. Leszczyński, S. Porowski, to be presented at *8th Int. Conf. on MOVPE, Cardif 1996.*

[3] S. Porowski, J. Jun, M. Boćkowski, M. Leszczyński, S. Krukowski, M. Wróblewski, B. Łucznik, I. Grzegory, in: *Proc. 8th Conf. on Semiinsulating III–V Materials*, Ed. M. Godlewski, World Scientific, Singapore 1994, p. 61.

[4] S. Porowski, J.M. Baranowski, M. Leszczyński, J. Jun, M. Boćkowski, I. Grzegory, S. Krukowski, M. Wróblewski, B. Łucznik, G. Nowak, K. Pakuła, A. Wysmołek, K.P. Korona, R. Stępniewski, in: *Proc. Int. Symp. on Blue Laser and Light Emiting Diodes, Chiba 1996*, Eds. A. Yoshikawa, K. Kishino, M. Kobayashi, T. Yasuda, Ohmsha Ltd., Tokyo 1996, p. 38.

[5] J.M. Baranowski, S. Porowski, in: *Proc. 9th Conf. on Semiinsulating III–V Materials, Toulouse 96*, to be published.

[6] M. Leszczyński, H. Teisseyre, T. Suski, I. Grzegory, M. Boćkowski, J. Jun, S. Porowski, K. Pakuła, J.M. Baranowski, C.T. Foxon, T.S. Cheng, submited to *Appl. Phys. Lett.*

[7] K. Pakuła, A. Wysmołek, K.P. Korona, J.M. Baranowski, R. Stępniewski, I. Grzegory, M. Boćkowski, J. Jun, S. Krukowski, M. Wróblewski, S. Porowski, *Solid State Commun.* **97**, 919 (1996).

[8] H. Schulz, K.H. Thiemann, *Solid State Commun.* **23**, 815 (1977).

[9] R.C. Powell, N.E. Lee, Y.W. Kim, J.E. Greene, *J. Appl. Phys.* **73**, 189 (1993).

[10] K. Miwa, A. Fukumoto, *Phys. Rev. B* **48**, 7897 (1993).

[11] I. Gorczyca, N.E. Christensen, *Solid State Commun.* **80**, 335 (1991).

[12] S. Logethetidis, J. Petlas, M. Cardona, T.D. Moustakas, *Phys. Rev. B* **50**, 18017 (1994).

[13] G. Ramirez-Flores, H. Navarro-Contreeas, A. Lastras-Martinez, R.C. Powell, J.E. Greene, *Phys. Rev. B* **50**, 8433 (1994).

[14] D.G. Thomas, J.J. Hopfield, *Phys. Rev.* **116**, 573 (1959).

[15] K.P. Korona, A. Wysmołek, K. Pakuła, R. Stępniewski, J.M. Baranowski, I. Grzegory, B. Łucznik, M. Wróblewski, S. Porowski, *Appl. Phys. Lett* **69**, 788 (1996).

[16] G.L. Bir, G.E. Pikus, *Symmetry and Strain-Induced Effects in Semiconductors*, John Wiley &Sons, New York 1974.

[17] B. Gil, O. Briot, R.L. Aulombard, *Phys. Rev. B* **52**, R17028 (1995).

[18] D. Volm, K. Oettinger, T. Streibl, D. Kovalev, M. Ben-Chorin, J. Diener, B.K. Meyer, J. Majewski, L. Eckey, A. Hoffman, H. Amano, I. Akasaki, *Phys. Rev. B* **53**, 16543 (1996).

[19] G. Mahler, U. Schröder, *Phys. Status Solidi B* **61**, 629 (1974).

[20] M. Drechsler, D.M. Hofmann, B.M. Meyer, T. Detchprochm, H. Amano, I. Akasaki, *Jpn. J. Appl. Phys.* **34**, L1178 (1995).

[21] W. Knap, H. Alause, J.M. Bluet, J. Camassel, J. Young, M. Asif Khan, Q. Chen, S. Huant, M. Shur, *Solid State Commun.* **99**, 195 (1996).

[22] A.S. Barker, Jr., M. Ilegems, *Phys. Rev. B* **7**, 743 (1973).

[23] A.M. Stoneham, *Theory of Defects in Solids*, Clarendon Press, Oxford 1975, Ch. 8.6.

[24] M. Sufczyński, L. Wolniewicz, *Phys. Rev B* **40**, 6250 (1989).

[25] A. Wysmołek, J.M. Baranowski, K. Pakuła, I. Grzegory, M. Wróblewski, S. Porowski, in: *Proc. Int. Symp. on Blue Laser and Light Emiting Diodes, Chiba 1996*, Ed. A. Yoshikawa, K. Kishino, M. Kobayashi, T. Yasuda, Ohmsha Ltd., Tokyo 1996, p. 492.

[26] R. Stępniewski, M. Potemski, A. Wysmołek, K. Pakuła, J.M. Baranowski, G. Martinez, I. Grzegory, M. Wróblewski, S. Porowski, to be presented at *23th Int. Conf. on Phys. of Semiconductors*, Berlin 1996.

[27] D.G. Thomas, J.J. Hopfield, *Phys. Rev.* **128**, 2135 (1962).

[28] W.E. Carlos, J.A. Freitas, Jr., M. Asif Khan, D.T. Olson, J.N. Kuznia, *Phys. Rev. B* **24**, 17878 (1993).

[29] M. Kunzer, U. Kaufmann, K. Maier, J. Schneider, N. Herres, I. Akasaki, H. Amano, *Mater. Sci. Forum* **143-147**, 87 (1994).

[30] M. Godlewski, A. Wysmołek, K. Pakuła, J.M. Baranowski, I. Grzegory, J. Jun, S. Porowski, J.P. Bergman, B. Monemar, in: *Proc. Int. Symp. on Blue Laser and Light Emiting Diodes, Chiba 1996*, Eds. A. Yoshikawa, K. Kishino, M. Kobayashi, T. Yasuda, Ohmsha Ltd., Tokyo 1996, p. 356.

[31] A. Wysmołek, K.P. Korona, P. Łomiak, K. Pakuła, J.M. Baranowski, R. Stępniewski, M. Godlewski, I. Grzegory, M. Boćkowski, S. Porowski, this conference, unpublished.

[32] A. Wysmołek, K.P. Korona, K. Pakuła, J.M. Baranowski, R. Stępniewski, I. Grzegory, M. Wróblewski, S. Porowski, to be presented at *23th Int. Conf. on Phys. of Semiconductors, Berlin 1996.*

[33] P. Bogusławski, E. Briggs, J. Bernholc, *Phys. Rev. B* **51**, 17255 (1995).